High-performance GaAs metal-oxide-semiconductor capacitor by using NbAlON as high-k gate dielectric

L. N. Liu,[1] H. W. Choi,[1] J. P. Xu,[2] and P. T. Lai[1,a)]
[1]*Department of Electrical and Electronic Engineering, the University of Hong Kong, Hong Kong 999077, Hong Kong*
[2]*School of Optical and Electronic Information, Huazhong University of Science and Technology, Wuhan, China*

(Received 6 October 2016; accepted 11 March 2017; published online 22 March 2017)

A GaAs metal-oxide-semiconductor (MOS) capacitor using NbAlON as a gate dielectric with different Nb contents is fabricated. Experimental results show that the k value and crystallization temperature of the AlON dielectric can be improved by Nb incorporation, together with reduction in negative oxide charges. However, the interface quality and gate leakage become poorer as the Nb content increases, as confirmed by TEM and X-ray photoelectron spectroscopy results. Therefore, through comprehensively considering the advantages and disadvantages, the sample with a Nb/(Al+Nb) atomic ratio of 62.5% exhibits the best characteristics: high k value (23.3), low interface-state density ($2.7 \times 10^{12}\,cm^{-2}/eV$), small hysteresis (55 mV), small frequency dispersion, and low gate leakage current ($2.66 \times 10^{-5}\,A/cm^2$ at $V_{fb} + 1\,V$). By comparing with reported GaAs MOS devices with different high-k gate dielectrics, it can be suggested that NbAlON is a promising gate dielectric material to achieve excellent electrical performance for GaAs MOS devices. *Published by AIP Publishing*. [http://dx.doi.org/10.1063/1.4979101]

In order to counteract the increasing degradation caused by Si-based metal-oxide-semiconductor (MOS) technology approaching its scaling limit and fulfill the requirements of higher performance and lower power consumption in the future, GaAs has received significant attention recently due to its higher electron mobility, larger bandgap, and higher breakdown field than those of Si.[1–3] For GaAs MOS devices, ideal gate dielectrics should possess (i) high dielectric constant (high-k), (ii) sufficient bandgap and band offset with the conduction band of GaAs, and (iii) thermal stability and low interface-state density (D_{it}) with GaAs.[4] Many high-k materials (e.g., HfO_2,[5] La_2O_3,[6] Y_2O_3,[7] and ZrO_2 (Ref. 8)) have been tried on GaAs with good results achieved, but (iii) is still challenging even now. In order to improve the quality of the high-k/GaAs interface, NH_3 or F treatment[9,10] and passivating interlayer (e.g., Si,[11] Ge,[12] Al_2O_3,[13] ZnO,[14] and TaLaON[15]) have been studied. However, the high D_{it} and the easily formed unstable native oxide of GaAs still need to be suppressed to avoid the Fermi-level pinning at the high-k/GaAs interface.[7] Moreover, it has been shown that the interface states tend to cause a severer impact on the n-type GaAs MOS device than on its p-type counterpart, leading to much larger frequency dispersion.[16] Therefore, improving the properties of the n-type GaAs MOS device is a bigger challenge in order to achieve GaAs CMOS applications.

Owing to a large bandgap (8.8 eV) and high breakdown field, Al_2O_3 has been proved to achieve a relatively good interface with GaAs[17] and its nitride (AlON) has been used for GaAs surface passivation[18] because nitrogen incorporation is known to reduce border traps and improve the k value of dielectrics.[19] However, the low k value (~9) and the high density of negative defects of Al_2O_3 bulk[20] are the factors that limit device scaling and cause a threshold-voltage shift, respectively. On the other hand, the high k value (>40) of Nb_2O_5 makes it achieve high capacitance density, and so a low-cost capacitor with Nb_2O_5 has long been considered as a replacement for Ta_2O_5 in the discrete-component industry.[21] Unfortunately, the small bandgap (3.4 eV) and high density of defects (e.g., oxygen vacancies) of Nb_2O_5 cause high leakage current and strong Coulomb scattering,[22] negatively impacting the carrier mobility and drive current of the MOS devices. Therefore, riding on the advantages of Al_2O_3 and Nb_2O_5, this work proposes an appropriate Nb/Al ratio in the NbAlON gate dielectric that achieves good interfacial, gate leakage properties and a relatively high k value for GaAs MOS applications by investigating the effects of Nb incorporation in AlON.

MOS capacitors were fabricated on Si-doped n-GaAs wafers (100) with a doping concentration of $(1–5)\times10^{17}\,cm^{-3}$. Wafers were first degreased in acetone, ethanol, and isopropanol sequentially and then dipped in diluted HCl to remove the native oxide, followed by dipping in 8% $(NH_4)_2S$ for 40 min for passivating the GaAs surface.[23] After drying with N_2, the wafers were transferred immediately into a high vacuum chamber of a sputtering system. The NbAlON gate dielectric (~10 nm) was then deposited by co-sputtering Nb and Al_2O_3 targets in an ambient of Ar/N_2 (24 sccm/12 sccm) at room temperature. Different Nb/Al ratios in the NbAlON film were obtained by adjusting the DC/RF powers of the Nb/Al_2O_3 targets to 0.08A/45W, 0.05A/45W, 0.02A/45W, and 0A/45W, denoted as samples A, B, C, and D, respectively. Subsequently, a post-deposition annealing (PDA) was carried out at 600 °C for 60 s in N_2 for all the samples. An Al electrode was then evaporated and patterned with an area of $7.85 \times 10^{-5}\,cm^2$, followed by a forming-gas (95% N_2 + 5% H_2) annealing at 300 °C for 20 min.

Capacitance-voltage (C-V) measurement was performed on the MOS capacitors by using a HP 4284A precision LCR

a)Email: laip@eee.hku.hk

meter. Gate leakage current was tested by using a HP 4156A semiconductor parameter analyzer, and the thickness of the dielectric films (T_{ox}) was measured by ellipsometry. Moreover, the chemical states in high-k bulks and at/near the high-k/GaAs interface were analyzed by X-ray photoelectron spectroscopy (XPS).

According to the XPS results which will be analyzed in detail below, the atomic ratio of Nb to (Al + Nb) can be extracted to be 90.6%, 62.5%, 45.7%, and 0% for the samples A, B, C, and D, respectively (extraction details are given in the supplementary material). The cross-sectional images of the four samples obtained by scanning TEM (FEI Tecnai G2 20, with an operating high tension of 200 kV) are shown in Fig. 1. An interfacial layer (IL), consisting of GaAs native oxides with thicknesses of 3.11 nm, 1.82 nm, and 1.76 nm for samples A, B, and C, respectively, can be clearly observed, indicating that the Nb incorporation promotes the oxidation of the GaAs surface due to enhanced O diffusion to the GaAs surface. In addition, the sign of crystallization appears in sample D but not in samples A, B, and C. It has been reported that compared with those prepared by other deposition methods (e.g., metal organic chemical vapor deposition (MOCVD)), Al_2O_3 deposited by sputtering is easier to crystallize at relatively low temperature.[24] Moreover, it is more difficult for multi-element high-k oxide to crystallize due to the stoichiometric issue. Therefore, only sample D without Nb incorporation shows slight crystal lines, leading to larger leakage current and possibly poorer interface with the GaAs substrate.

The 1-MHz C-V curves of the samples swept from inversion to accumulation and then back are shown in Fig. 2(a). The clockwise hysteresis of the samples decreases with the decreasing Nb concentration, implying a reduction of the capture of electrons by acceptor-like traps formed through the oxygen vacancies in Nb_2O_5.[25] Obviously, the accumulation capacitance per unit area (C_{ox}) increases with the increasing Nb content due to the much higher k value of Nb_2O_5 than that of Al_2O_3. However, the largest stretch out of the C-V curve and a breakdown at high gate voltage are found for sample A (Nb content of 90.6%) with the largest C_{ox} imply its worst interface and dielectric qualities. Many studies have been made on extracting the interface-state density near mid-gap (D_{it}).[26–28] In this work, D_{it} is extracted by Terman's method (based on the HF C-V curve)[29] and the conductance-voltage method[30] (extraction methodology is given in the supplementary material) and is shown in Fig. 2(b), which is consistent with the IL shown in Fig. 1: the thicker the IL, the higher is the interface-state density when comparing samples A, B, and C. The higher D_{it} of sample D than that of samples B and C should be caused by the slight crystallization of AlON.

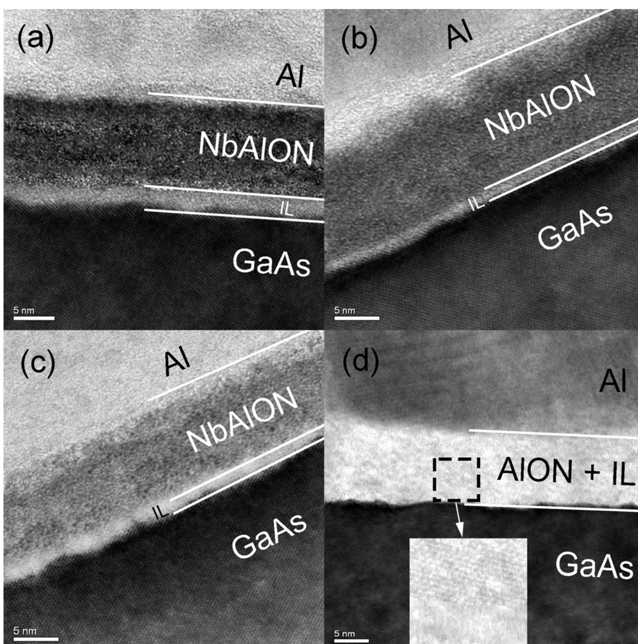

FIG. 1. Cross-sectional TEM image of Al/NbAlON/GaAs gate stacks with different Nb/Al ratios: (a) sample A (90.6%), (b) sample B (62.5%), (c) sample C (45.7%), and (d) sample D (0%).

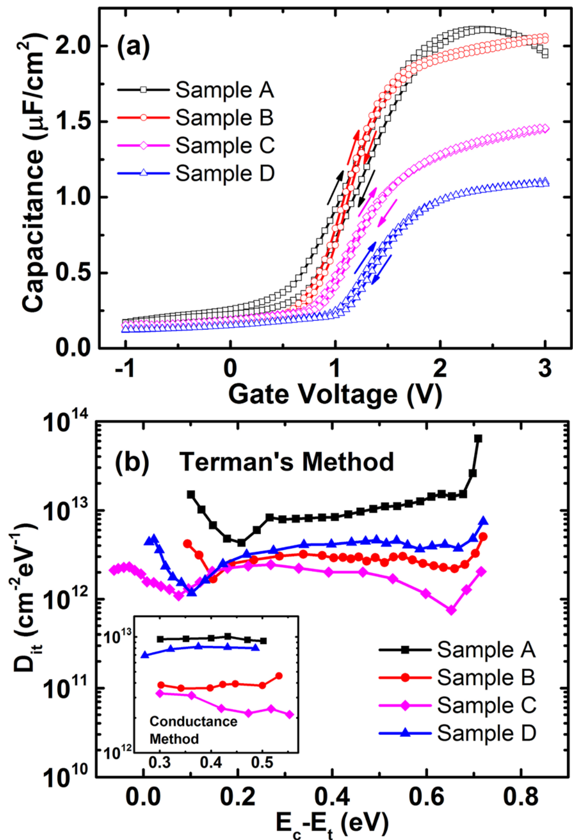

FIG. 2. (a) High-frequency C-V curve and (b) interface-state density in the bandgap.

The electrical and physical parameters of the samples extracted from their HF C-V curves are listed in Table I. The equivalent k value of the gate dielectrics can be calculated by $k = k_{SiO2}T_{ox}/CET$, where CET (capacitance equivalent thickness) equals $k_0 k_{SiO2}/C_{ox}$ (k_0 is the vacuum permittivity; k_{SiO2} is the dielectric constant of SiO_2). Flatband voltage V_{fb} is determined from flatband capacitance, and thus the equivalent oxide-charge density (Q_{ox}) can be obtained by $-C_{ox}(V_{fb} - \varphi_{ms})/q$, in which φ_{ms} is the work-function difference between the Al gate and GaAs substrate and q is the electron charge. Positive V_{fb} for all the samples implies the presence of negative charges in the dielectric film since reports show that the dominant fixed charges in bulk Al_2O_3 are negative.[31] V_{fb} decreases from 1.38 V (sample D) to 1.08 V (sample B), implying that the amount of negative fixed charges is reduced with the decreasing Al content. However, the

TABLE I. Electrical and physical parameters of the samples.

Sample no.	A	B	C	D
Nb/(Al+Nb) (%)	90.6	62.5	45.7	0
T_{ox} (nm)	10.06	10.02	10.26	10.13
C_{ox} (μF/cm^2)	2.11	2.06	1.45	1.10
V_{fb} (V)	1.10	1.08	1.21	1.38
Q_{ox} (cm^{-2})	-1.25×10^{13}	-1.21×10^{13}	-9.87×10^{12}	-8.42×10^{12}
CET (nm)	1.64	1.67	2.38	3.14
K	23.9	23.3	16.8	12.5
Hysteresis (mV)	145	55	45	40

increased V_{fb} of sample A (1.10 V) should be related to the larger stretch-out in the C-V curve caused by its larger D_{it} (Fig. 2(b)) that makes it reach the flatband capacitance slower. Moreover, although sample A has 28.1% more Nb than sample B, its k value is only 0.6 larger than that of sample B, which should be ascribed to the thicker low-k IL in sample A as shown by the TEM results in Fig. 1.

The C-V curves of the samples measured from 500 Hz to 1 MHz are displayed in Fig. 3. Interface traps cause the frequency dispersion in the transition region, while inhomogeneous layers formed at the gate-dielectric/substrate interface, high gate leakage, and oxide degradation are the reasons for the dispersion in the accumulation region.[32,33] Therefore, the poor C-V behavior at low frequency for the samples A and D in the transition region indicates higher density of interface states,[34] and the largest C_{ox} increment for sample A is possibly due to its thickest IL layer. Smaller frequency dispersion is obtained for samples B and C, consistent with their smaller D_{it} in Fig. 2(b), thus supporting that an appropriate amount of Nb in the high-k dielectric is capable of optimizing the interface quality in this study.

Fig. 4(a) shows the gate leakage current density vs. voltage ($J_g - V_g$) curve of the four samples. Samples B and C exhibit much lower gate leakage (2.66×10^{-5} A/cm^2 and 1.78×10^{-5} A/cm^2, respectively, at $V_g = V_{fb} + 1$ V) than sample A (slight breakdown at $\sim$2 V), which should be ascribed to their smaller amount of oxide/interface traps (causing trap-assisted tunneling[35]) and much larger bandgap of Al_2O_3 (than that of Nb_2O_5). Sample D shows the lowest gate leakage in the low-voltage

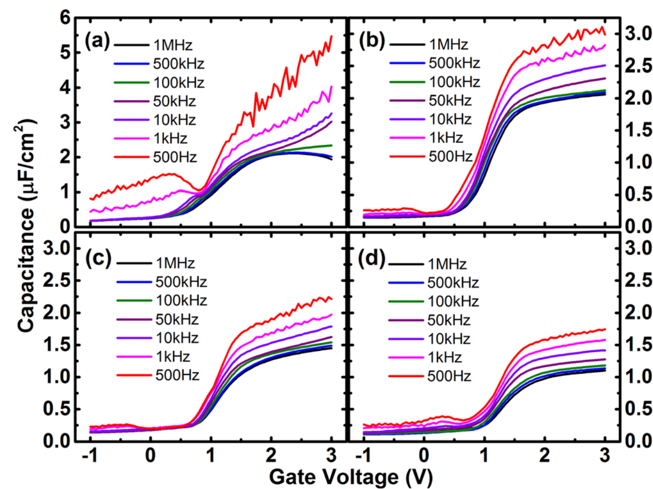

FIG. 3. Frequency dispersion of the C-V curve: (a) sample A, (b) sample B, (c) sample C, and (d) sample D.

regime but exceeds that of sample C in the high-voltage region, which should be due to the crystallization of AlON as mentioned above. The Fowler-Nordheim tunneling model is used to extract the conduction-band offset between the dielectric and GaAs substrate, with the result shown in the inset of Fig. 4(a) (details are given in the supplementary material). After Nb incorporation, the band offset decreases, consistent with the fact that Nb_2O_5 has a smaller band gap than Al_2O_3.

A stress of 3MV/cm ((V_g-V_{fb})/T_{ox}) for 3600 s is applied on the samples with gate leakage measured every 600 s for reliability evaluation, and their leakage current density increments (ΔJ_g) at $V_{fb} + 1$ V are compared in Fig. 4(b). A monotonic increase in ΔJ_g can be found in all the samples because the amount of electrons tunneling from the substrate to the gate increases through the newly generated interface states and the pre-existing states near the interface.[18] Once again, the smaller ΔJ_g of samples B and C than that of samples A and D is in good agreement with their D_{it}s in Fig. 2(b). Therefore, it can be concluded that sample B exhibits smaller frequency dispersion, better device reliability, smaller hysteresis, and lower D_{it} and gate leakage than sample A due to a better-quality dielectric film and a high-k/GaAs interface, despite a slight loss in the k value. Moreover, the much higher k value of sample B with comparable dielectric and interface qualities to sample C suggests that the Nb content of 62.5% is preferred. Also, in Table II, a comparison between sample B and some recently reported metal/high-k/n-GaAs devices with relatively good performance (without interfacial passivation and with the dielectric prepared by the sputtering method for fair comparison) indicates that NbAlON is a promising gate dielectric for high-performance GaAs MOS devices. Since NbAlO has been demonstrated as a promising high-k dielectric for the InP MOS device,[40,41] it is possible that the C-V stretch-out, hysteresis, and gate leakage could be improved by using a more appropriate Nb/Al ratio to achieve higher bulk and interfacial qualities for the gate dielectric.

The Al 2p and Nb 3d XPS spectra in the dielectric bulk are analyzed in Fig. 5 for supporting their electrical properties. Al-N and Nb-N bonds can be detected together with Al-O and Nb-O bonds due to the nitrogen incorporation, and the suboxide peaks are caused by the insufficient oxidation of Nb and Al. The oxygen vacancies in high-k oxide films are frequently reported to be positive,[42,43] so binding energies tend to shift to lower levels if the amount of oxygen vacancies decreases because the core-level binding energy of an atom increases with a positive charge nearby.[44] Therefore, using the C 1s peak at 284.6 eV as a reference (adventitious C from inevitable contamination), the shift of both Al 2p and Nb 3d to lower binding energies as the Al content increases demonstrates a decrease in oxygen vacancies in the dielectric film, indicating that Al can effectively passivate the oxygen vacancies in Nb_2O_5, just like passivating the oxygen vacancies in HfO_2 by shifting the vacancy gap states up into the conduction band.[45]

After the gate dielectric is etched by an *in situ* Ar^+ ion beam, chemical states at/near the high-k/GaAs interface of the samples are also analyzed by XPS. The As 3d and Ga 3d XPS spectra of the samples are compared in Fig. 6. Peaks of As-Ga, As-As, As-S, and As-O bonds are detected at 41.7 eV, 42.2 eV, 42.9 eV, and 44.6 eV, respectively, in Fig. 6(a), and in Fig. 6(b), the peaks located at 18.7 eV, 19.5 eV,

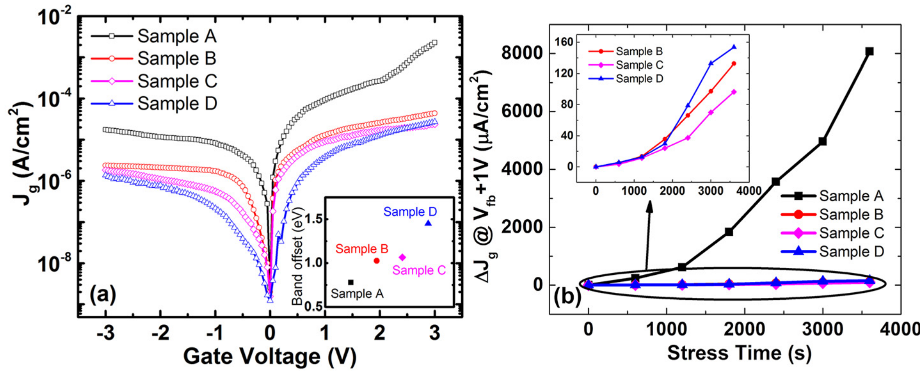

FIG. 4. (a) J_g-V_g characteristics and (b) ΔJ_g vs. stress time for the samples.

TABLE II. Electrical properties of GaAs MOS capacitors with different high-k dielectrics deposited by sputtering.

	T_{ox} (nm)	k value	CET (nm)	D_{it} (10^{12} cm^{-2} eV^{-1})	Hysteresis (mV)	J_g (A/cm^2) @ V_{fb}+1V
TaAlO[36]	10.0	12.0	2.9	4.3	670	2.3×10^{-4}
HfTiON[18]	11.4	24.7	1.8	5.4	70	8.3×10^{-4}
TaYON[15]	10.9	18.1	2.3	3.0	90	4.2×10^{-4}
HfAlO[37]	10.0	13.0	2.1	6.2	550	1.9×10^{-4}
ZrON[38]	10.0	9.8	3.9	8.9	80	6.6×10^{-3}
HfO_2[39]	22.0	18.0	4.4	9.5	800	2.3×10^{-3}
This work	10.0	23.3	1.6	2.7	55	2.6×10^{-5}

and 20.8 eV correspond to Ga-As, Ga-S, and Ga-O bonds, respectively, according to the National Institute of Standards and Technology (NIST) XPS database. With a wide range of binding energies, As and Ga sub-oxide peaks should also be included in the As-S, As-As, and Ga-S peaks. By comparing

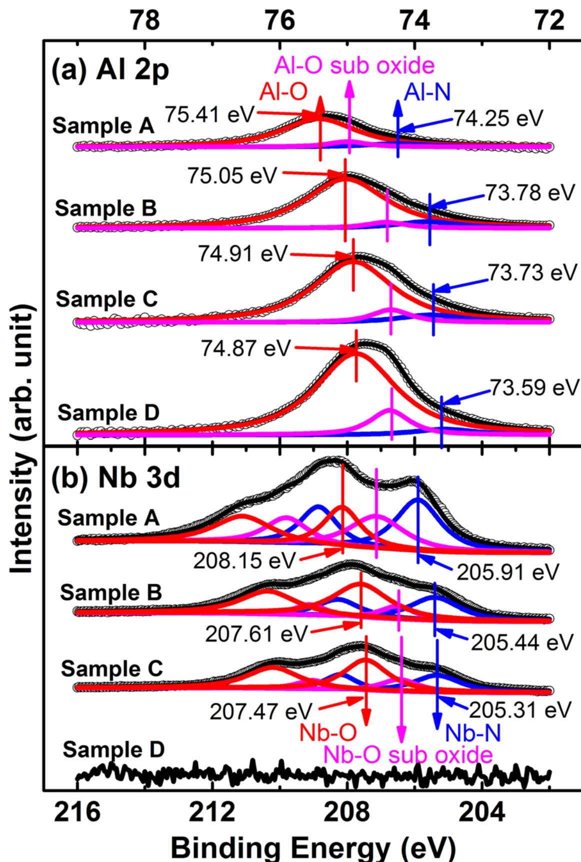

FIG. 5. XPS spectrum for the dielectric bulk of the samples: (a) Al 2p and (b) Nb 3d.

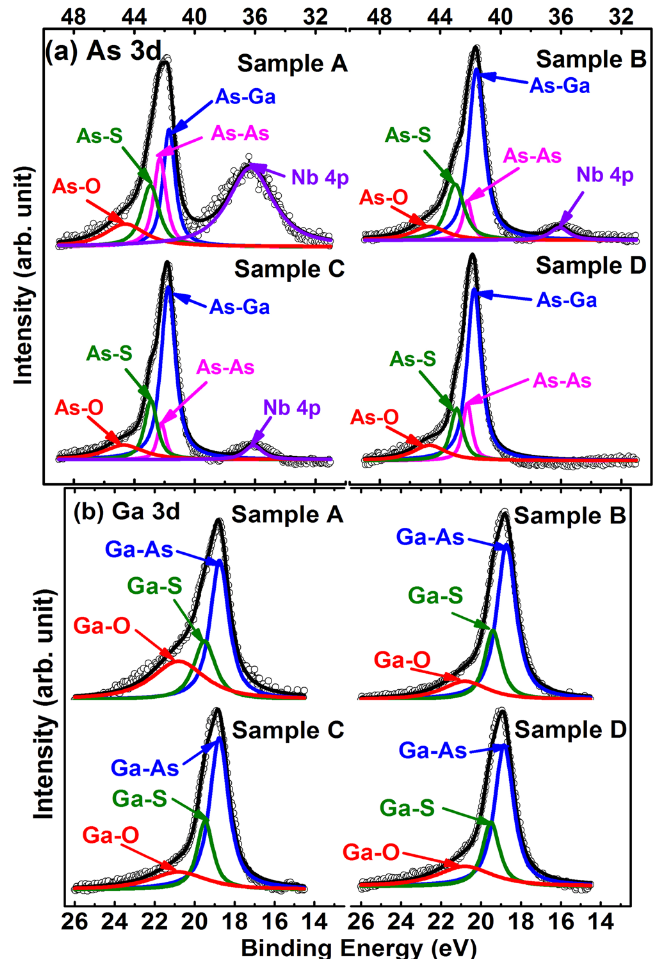

FIG. 6. XPS spectrum at/near the high-k/GaAs interface: (a) As 3d and (b) Ga 3d.

samples A, B, and C, the peaks of unstable As-As, As-O bonds in Fig. 6(a) and Ga-O bonds in Fig. 6(b) are weakened with the decrease in the Nb content (peaks comparable for samples B and C), consistent with the results on electrical properties (Table I) and interfacial layer (Fig. 1), indicating that the decrease in interface traps exhibits a saturation tendency as the Nb content decreases (see Fig. 2(b)). This is also consistent with the fact that O can strongly bond with Al. Therefore, as the Nb concentration increases, the Al content is decreased in NbAlON and so less Al is available for bonding with O, thus promoting the O diffusion.

In addition, Nb 4p can be detected at 36.3 eV at/near the interface of samples A, B, and C due to the diffusion of Nb from the dielectric to the substrate (Fig. 6(a)). The strongest Nb peak with a content of 43.7% in sample A is another reason that causes its largest D_{it}. The significantly weakened Nb 4p peak in samples B and C (with the Nb-O bond content of 5.7% and 5.1%, respectively) contributes to the decrease in interface states (see Fig. 2(b)), thus improving the electrical properties of the device.

The effects of Nb doping in the NbAlON gate dielectric on the performance of the GaAs MOS capacitor are investigated. With Nb incorporation, the k value of the gate dielectric is greatly increased, but trade-off exists because oxygen vacancies, interface states, and the thickness of the low-k interfacial layer are also increased. Moreover, the negative fixed charges in the AlON decrease with the increasing Nb content and thus reduce V_{fb}. The diffusion of Nb from the dielectric to the substrate gets stronger with the increase in the Nb content, leading to a larger deterioration in the interface quality. Accordingly, the sample with a Nb/(Al+Nb) ratio of 62.5% exhibits the best properties: thin low-k interfacial layer, small hysteresis, good high-field reliability, low interface-state density, small leakage current, and large k value. In summary, NbAlON with an optimal Nb/Al ratio is a promising gate dielectric to achieve high-performance GaAs MOS devices.

See supplementary material for details of the band offset between the high-k dielectric and GaAs conduction band, D_{it} extraction, XPS analysis, and supplementary XPS spectra.

This work was financially supported by University Development Fund (Nanotechnology Research Institute, 00600009) of the University of Hong Kong and the National Natural Science Foundation of China (Grant Nos. 61176100 and 61274112).

[1]C. P. Chen, Y. J. Lee, Y. C. Chang, Z. K. Yang, M. Hong, J. Kwo, H. Y. Lee, and Y. S. Lay, J. Appl. Phys. **100**, 104502 (2006).
[2]Y. C. Chang, C. Merckling, J. Penaud, C. Y. Lu, W. E. Wang, J. Dekoster, M. Meuris, M. Caymax, M. Heyns, J. Kwo, and M. Hong, Appl. Phys. Lett. **97**, 112901 (2010).
[3]P. Kordos, R. Kudela, R. Stoklas, K. Cico, M. Mikulics, D. Gregusova, and J. Novak, Appl. Phys. Lett. **100**, 142113 (2012).
[4]R. Engel-Herbert, Y. Hwang, and S. Stemmer, J. Appl. Phys. **108**, 124101 (2010).
[5]D. Shahrjerdi, D. I. Garcia-Gutierrez, T. Akyol, S. R. Bank, E. Tutuc, J. C. Lee, and S. K. Banerjee, Appl. Phys. Lett. **91**, 193503 (2007).
[6]T. Das, C. Mahata, C. K. Maiti, G. K. Dalapati, C. K. Chia, D. Z. Chi, S. Y. CHiam, H. L. Seng, C. C. Tan, H. K. Hui, G. Sutradhar, and P. K. Bose, J. Electrochem, Soc. **159**, G15 (2012).
[7]Y. H. Lin, C. H. Fu, K. Y. Lin, K. H. Chen, T. W. Chang, J. R. Kwo, and M. H. Hong, Appl. Phys. Express **9**, 081501 (2016).
[8]K. Kundu, S. Roy, P. Banerji, S. Chakraborty, and T. Shripathi, J. Vac. Sci. Technol., B **29**, 031203 (2011).
[9]H. H. Lu, J. P. Xu, L. Liu, L. S. Wang, P. T. Lai, and W. M. Tang, Microelectron. Reliab. **56**, 17 (2016).
[10]L. N. Liu, H. W. Choi, J. P. Xu, and P. T. Lai, J. Vac. Sci. Technol., B **33**, 050601 (2015).
[11]S. Koveshnilcov, W. Tsai, I. Ok, J. C. Lee, V. Torkanov, M. Yaldmov, and S. Oktyabrsky, Appl. Phys. Lett. **88**, 022106 (2006).
[12]D. Shahrjerdi, M. M. Oye, A. L. Holmes, Jr., and S. K. Banerjee, Appl. Phys. Lett. **89**, 043501 (2006).
[13]M. M. Frank, G. D. Wilk, D. Starodub, T. Gustafsson, E. Garfunkel, Y. J. Chabal, J. Grazul, and D. A. Muller, Appl. Phys. Lett. **86**, 152904 (2005).
[14]Y. C. Byun, S. Choi, Y. An, P. C. McIntyre, and H. Kim, ACS Appl. Mater. Interfaces **6**, 10482 (2014).
[15]L. N. Liu, H. W. Choi, J. P. Xu, and P. T. Lai, Appl. Phys. Lett. **107**, 213501 (2015).
[16]C. L. Hinkle, A. M. Sonnet, M. Milojevic, F. S. Aguirre-Tostado, H. C. Kim, J. Kim, R. M. Wallace, and E. M. Vogel, Appl. Phys. Lett. **93**, 113506 (2008).
[17]D. C. Suh, Y. D. Cho, S. W. Kim, D. H. Ko, Y. Lee, M. H. Cho, and J. Oh, Appl. Phys. Lett. **96**, 142112 (2010).
[18]L. S. Wang, L. Liu, J. P. Xu, S. Y. Zhu, Y. Huang, and P. T. Lai, IEEE Trans. Electron Devices **61**, 742 (2014).
[19]L. M. Lin and P. T. Lai, J. Mater. Sci.:Mater. Electron. **19**, 894 (2008).
[20]J. J. H. Gielis, B. Hoex, M. C. M. van de Sanden, and W. M. M. Kessels, J. Appl. Phys. **104**, 073701 (2008).
[21]S. J. Kim, B. J. Cho, M. B. Yu, M. F. Li, Y. Z. Xiong, C. Zhu, A. Chin, and D. L. Kwong, IEEE Electron Device Lett. **26**, 625 (2005).
[22]J. Sikula, J. Hlavka, V. Sedlakova, L. Grmela, P. Hoeschl, T. Zednlcek, and Z. Sita, “Conductivity mechanisms and breakdown characteristics of niobium oxide capacitors,” Fountain Inn, SC, USA, 2003, http://www.mouser.com/pdfdocs/CondNbO.pdf.
[23]E. O’Connor, B. Brennan, V. Djara, K. Cherkaoui, S. Monaghan, S. B. Newcomb, R. Contreras, M. Milojevic, G. Hughes, M. E. Pemble, R. M. Wallace, and P. K. Hurley, J. Appl. Phys. **109**, 024101 (2011).
[24]P. Jin, S. Nakao, S. X. Wang, and L. M. Wang, Appl. Phys. Lett. **82**, 1024 (2003).
[25]K. Tse, D. Liu, K. Xiong, and J. Robertson, Microelectron. Eng. **84**, 2028 (2007).
[26]G. Brammertz, H. C. Lin, K. Martens, D. Mercier, S. Sioncke, A. Delabie, W. E. Wang, M. Caymax, M. Meuries, and M. Heyns, Appl. Phys. Lett. **93**, 183504 (2008).
[27]K. Marten, C. O. Chui, G. Brammertz, B. D. Jaeger, D. Kuzum, M. Meuris, M. M. Heyns, T. Krishnamohan, K. Sarawat, H. E. Maes, and G. Groeseneken, IEEE Trans. Electron Devices **55**, 547 (2008).
[28]G. Brammertz, K. Martens, S. Sioncke, A. Delabie, M. Caymax, M. Meuris, and M. Heyns, Appl. Phys. Lett. **91**, 133510 (2007).
[29]L. M. Terman, Solid State Electron. **5**, 285 (1962).
[30]E. H. Nicollian and A. Goetzberger, Bell Syst. Tech. J. **46**, 1055 (1967).
[31]D. K. Simon, P. M. Jordan, T. Mikolajick, and I. Dirnstorfer, ACS Appl. Mater. Interfaces **7**, 28215 (2015).
[32]G. K. Dalapati, Y. Tong, W. Y. Loh, H. K. Mun, and Y. J. Cho, Appl. Phys. Lett. **90**, 183510 (2007).
[33]G. K. Dalapati, Y. Tong, W. Y. Loh, H. K. Mun, and Y. J. Cho, IEEE Trans. Electron Devices **54**, 1831 (2007).
[34]K. Marten, W. Wang, K. De Deersmaecker, G. Borghs, G. Groeseneken, and H. Maes, Microelectron. Eng. **84**, 2146 (2007).
[35]F. Gao, S. J. Lee, D. Z. Chi, S. Balakumar, and D. L. Kwong, Appl. Phys. Lett. **90**, 252904 (2007).
[36]P. S. Das and A. Biswas, Appl. Phys. A **118**, 967 (2015).
[37]P. S. Das and A. Biswas, Appl. Surf. Sci. **256**, 6618 (2010).
[38]H. H. Lu, J. P. Xu, and L. Liu, IEEE Trans. Device Mater. Reliab. **16**, 617 (2016).
[39]G. K. Dalapati, A. Sridhara, A. S. W. Wong, C. K. Chia, and D. Z. Chi, ECS Trans. **16**, 387 (2008).
[40]D. He, X. Cheng, D. Xu, Z. Wang, and Y. Yu, J. Vac. Sci. Technol., B **29**, 01A803 (2011).
[41]X. Cheng, D. Xu, Q. Sun, D. He, Z. Wang, Y. Yu, D. W. Zhang, and Q. Zhao, Appl. Phys. Lett. **96**, 022904 (2010).
[42]T. L. Duan, H. Y. Yu, L. Wu, Z. R. Wang, Y. L. Foo, and J. S. Pan, Appl. Phys. Lett. **99**, 012902 (2011).
[43]S. Guha and V. Narayanan, Phys. Rev. Lett. **98**, 196101 (2007).
[44]P. S. Bagus, F. Illas, G. Pacchioni, and F. Pamigiani, J. Electron. Spectrosc. **100**, 215 (1999).
[45]D. Liu and J. Robertson, Appl. Phys. Lett. **94**, 042904 (2009).